NASA/CR-1998-208962

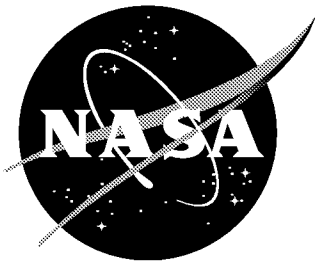

Closed Form Equations for the Preliminary Design of a Heat-Pipe-Cooled Leading Edge

David E. Glass
Analytical Services & Materials, Inc., Hampton, VA

December 1998

The NASA STI Program Office ... in Profile

Since its founding, NASA has been dedicated to the advancement of aeronautics and space science. The NASA Scientific and Technical Information (STI) Program Office plays a key part in helping NASA maintain this important role.

The NASA STI Program Office is operated by Langley Research Center, the lead center for NASA's scientific and technical information. The NASA STI Program Office provides access to the NASA STI Database, the largest collection of aeronautical and space science STI in the world. The Program Office is also NASA's institutional mechanism for disseminating the results of its research and development activities. These results are published by NASA in the NASA STI Report Series, which includes the following report types:

- TECHNICAL PUBLICATION. Reports of completed research or a major significant phase of research that present the results of NASA programs and include extensive data or theoretical analysis. Includes compilations of significant scientific and technical data and information deemed to be of continuing reference value. NASA counterpart of peer-reviewed formal professional papers, but having less stringent limitations on manuscript length and extent of graphic presentations.

- TECHNICAL MEMORANDUM. Scientific and technical findings that are preliminary or of specialized interest, e.g., quick release reports, working papers, and bibliographies that contain minimal annotation. Does not contain extensive analysis.

- CONTRACTOR REPORT. Scientific and technical findings by NASA-sponsored contractors and grantees.

- CONFERENCE PUBLICATION. Collected papers from scientific and technical conferences, symposia, seminars, or other meetings sponsored or co-sponsored by NASA.

- SPECIAL PUBLICATION. Scientific, technical, or historical information from NASA programs, projects, and missions, often concerned with subjects having substantial public interest.

- TECHNICAL TRANSLATION. English-language translations of foreign scientific and technical material pertinent to NASA's mission.

Specialized services that complement the STI Program Office's diverse offerings include creating custom thesauri, building customized databases, organizing and publishing research results ... even providing videos.

For more information about the NASA STI Program Office, see the following:

- Access the NASA STI Program Home Page at ***http://www.sti.nasa.gov***

- E-mail your question via the Internet to help@sti.nasa.gov

- Fax your question to the NASA STI Help Desk at (301) 621-0134

- Phone the NASA STI Help Desk at (301) 621-0390

- Write to:
  NASA STI Help Desk
  NASA Center for AeroSpace Information
  7121 Standard Drive
  Hanover, MD 21076-1320

NASA/CR-1998-208962

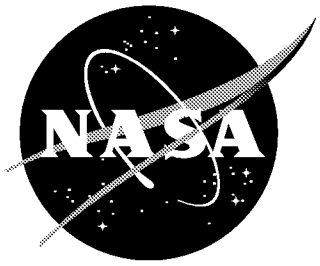

Closed Form Equations for the Preliminary Design of a Heat-Pipe-Cooled Leading Edge

David E. Glass
Analytical Services & Materials, Inc., Hampton, VA

National Aeronautics and
Space Administration

Langley Research Center
Hampton, Virginia 23681-2199

Prepared for Langley Research Center
under Contract NAS1-96014

December 1998

The use of trademarks or names of manufacturers in this report is for accurate reporting and does not constitute an official endorsement, either expressed or implied, of such products or manufacturers by the National Aeronautics and Space Administration or by Analytical Services & Materials, Inc.

Available from:

NASA Center for AeroSpace Information (CASI)
7121 Standard Drive
Hanover, MD 21076-1320
(301) 621-0390

National Technical Information Service (NTIS)
5285 Port Royal Road
Springfield, VA 22161-2171
(703) 605-6000

Available electronically at the following URL address: http://techreports.larc.nasa.gov/ltrs

Closed-Form Equations for the Preliminary Design of a Heat-Pipe-Cooled Leading Edge

David E. Glass
Analytical Services & Materials, Inc., Hampton, VA 23666
Phone: (757) 864-5423, e-mail: d.e.glass@larc.nasa.gov

Abstract

A set of closed form equations for the preliminary evaluation and design of a heat-pipe-cooled leading edge is presented. The set of equations can provide a leading-edge designer with a quick evaluation of the feasibility of using heat-pipe cooling. The heat pipes can be embedded in a metallic or composite structure. The maximum heat flux, total integrated heat load, and thermal properties of the structure and heat-pipe container are required input. The heat-pipe operating temperature, maximum surface temperature, heat-pipe length, and heat pipe-spacing can be estimated. Results using the design equations compared well with those from a 3-D finite element analysis for both a large and small radius leading edge.

Nomenclature

English

A	area, in^2
B	parameter utilized for grid transformation, in.
h	heat transfer coefficient for contact resistance, Btu/hr-ft^2-°F
k	thermal conductivity, Btu/hr-ft-°F
L	heat-pipe length, in.
p	equally spaced coordinates
q	heat flux, Btu/s
q"	heat flux per unit area, Btu/ft^2-s
r	leading-edge radius, in.
R	thermal resistance, hr-ft^2-°F/Btu
s	heat-pipe length, in.
t	thickness, in.
T	temperature, °F
w	width of heat pipe, in.
x	half heat-pipe spacing, in.
y	transformed coordinate for grid transformation, in.
z	point about which grid clustering occurs, in.

Greek

ε	emittance
σ	Stefan Boltzmann constant
Σ	summation
τ	stretching parameter for grid transformation

Subscripts and superscripts

amb	ambient
anal	obtained from 1-D closed-form design equations
avg	average
c	coating
cr	contact resistance
FEA	finite element analysis
hp	heat pipe
L	lower
max	maximum
s,hp	difference between structure and heat pipe temperature
s,t	structure property, through-the-thickness direction
s,p	structure property, in plane direction
stag	stagnation
surf	surface
tot	total
U	upper
w	heat-pipe wall

Introduction

Stagnation regions, such as wing and tail leading edges and nose caps, are critical design areas of hypersonic aerospace vehicles because of the hostile thermal environment those regions experience during flight. As a hypersonic vehicle travels through the earth's atmosphere, the high local heating and aerodynamic forces cause very high temperatures, severe thermal gradients, and high thermal stresses. Analytical studies, laboratory, and wind tunnel tests indicate that a solution to the thermal-structural problems associated with stagnation regions of hypersonic aerospace vehicles might be obtained by the use of heat pipes to cool these regions.

In the early 1970's, several feasibility studies were performed to assess the application of heat pipes for cooling leading edges and nose caps of hypersonic vehicles.[1-5] NASA Langley Research Center (LaRC), through a contractual study, analytically verified the viability of heat pipes for cooling stagnation regions of hypersonic vehicles.[1] In 1972, McDonnell Douglas Astronautics Co. (MDAC) compared four space shuttle wing leading-edge concepts: a passive carbon-carbon concept, a passive coated-columbium concept, an ablative concept, and a liquid-metal/superalloy heat-pipe-cooled concept.[2] The heat-pipe-cooled concept was determined to be a feasible and durable design concept, but was slightly heavier than the other candidate concepts. In 1973, MDAC fabricated a half-scale shuttle-type heat-pipe-cooled leading edge to verify feasibility of the concept.[4] This model was tested by a series of radiant heating and aerothermal tests at NASA LaRC from 1977 to 1978 to verify heat-pipe transient, startup, and steady-state performance.[6-8] In 1979, MDAC received a follow-on contract to optimize a heat-pipe-cooled wing leading edge for a single-stage-to-orbit vehicle. Results of the follow-on study indicated that the mass of a shuttle-type heat-pipe-cooled leading edge could be reduced by over 40% by use of a more efficient structural design.[9] In 1986 MDAC received a contract to design and fabricate a sodium/superalloy heat-pipe-cooled leading edge component for an advanced shuttle-type vehicle.[10] This advanced shuttle-type heat pipe was 6-ft long and was tested at MDAC by radiant heating and at Los Alamos National Laboratory (LANL) by induction heating.[11-12]

Preliminary design studies at NASA LaRC indicate that a refractory-composite/refractory-metal heat-pipe-cooled leading edge can reduce the leading-edge mass by over 50% compared to an actively cooled leading edge, can completely eliminate the

need for active cooling, and has the potential to provide failsafe and redundant features.[13] Recent work to develop this novel refractory-composite/refractory-metal heat-pipe-cooled leading edge for hypersonic vehicles combines advanced high-temperature materials, coatings, and fabrication techniques with an innovative thermal-structural design. Testing of a component at NASA LaRC with three straight molybdenum-rhenium (Mo-Re) heat pipes embedded in carbon/carbon (C/C) has demonstrated the feasibility of operating heat pipes embedded in C/C.[14-15]

When confronted with a leading-edge design for hypersonic vehicles, the options are passive, heat-pipe cooled, or actively cooled. The upper use limit for passive leading edges may be determined by evaluating the material properties in light of the thermal and mechanical loads. If passive leading edges cannot survive the environmental conditions, heat-pipe cooled or actively cooled leading edges will be required. Though heat pipes are often a viable and light weight option, the analysis required to determine if heat pipes are feasible for a particular application can be extensive and may thus preclude their use. It is thus beneficial to have a simple set of closed form equations that can be used to determine if the heat-pipe option is feasible. Having a simple analysis available may prevent the unnecessary use of active cooling when heat-pipes may provide a cheaper and lighter weight alternative and may prevent the unnecessary use of complex, 3D finite element analysis techniques to answer the question of initial feasibility, thus saving substantial analysis time.

The purpose of this paper is to present a set of simple, closed-form design equations that can be used to determine the feasibility of using a heat-pipe-cooled leading edge. The design equations presented here are only for thermal design, and do not include any stress analysis. Temperatures obtained from the design equations are compared to a 3-D finite element analysis for both a large and small leading-edge radius. Though some restrictions apply to the use of the equations, they appear to be a useful tool for a preliminary look at the feasibility of heat-pipe-cooled leading edges. If the preliminary design equations indicate a feasible design, a more detailed analysis should follow.

Description of Heat-Pipe-Cooled Leading-Edge

A brief description of how heat pipes operate and are utilized for leading-edge cooling is first presented, followed by a brief description of the heat-pipe-cooled leading-edge for which the equations were developed.

Leading-Edge Heat-Pipe Operation

Heat pipes transfer heat nearly isothermally by the evaporation and condensation of a working fluid, as illustrated in Figure 1. The heat is absorbed within the heat pipe by evaporation of the working fluid. The evaporation results in a slight internal pressure differential that causes the vapor to flow from the evaporator region to the condenser region, where it condenses and gives up heat. The cycle is completed with the return flow of the liquid condensate to the evaporator region by the capillary action of a wick.

Heat pipes provide cooling of stagnation regions by transferring heat nearly isothermally to locations aft of the stagnation region, thus raising the temperature aft of the stagnation region above the expected radiation equilibrium temperature. When applied to leading-edge cooling, heat pipes operate by accepting heat at a high rate over a small area near the stagnation region and radiating it at a lower rate over a larger surface area, as shown in Figure 2. The use of heat pipes results in a nearly isothermal leading-edge

surface, thus reducing the temperatures in the stagnation region and raising the temperatures of both the upper and lower aft surfaces.

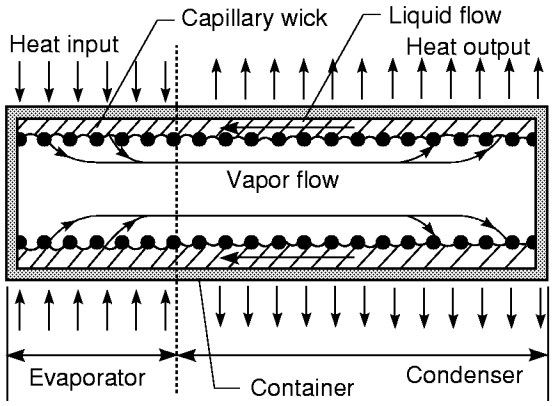

Figure 1: Schematic diagram of the operation of a heat pipe showing the heat-pipe container, working fluid, and wick.

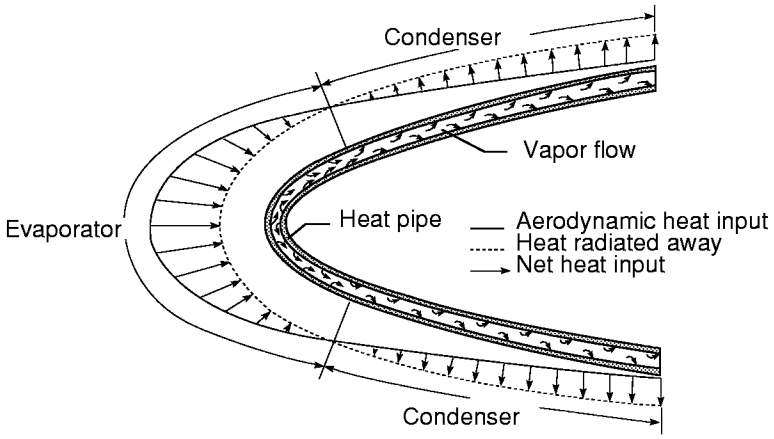

Figure 2: Schematic diagram of a heat-pipe-cooled leading edge showing regions of net heat input (evaporator) and net heat output (condenser).

Refractory Composite Heat-Pipe-Cooled Wing-Leading-Edge

The refractory composite heat-pipe-cooled wing leading edge for which the design equations were developed is illustrated in Figure 3. The heat pipes are oriented normal to the leading edge and have a "D-shaped" cross section, with the flat part of the "D" forming the wing-leading-edge outer surface. As shown in Figure 3, the leading edge contains "J-tube" heat pipes, with a "J-tube" heat pipe being a heat pipe with a long leg on one side of the nose region, and a short leg on the other side of the nose region. An alternating "J-tube" configuration was selected here to minimize heat-pipe spacing in the nose region where heating is the highest, provide a greater heat-pipe spacing on the upper and lower surfaces where heating is lower, and, at the same time, minimize mass. The refractory composite structure sustains most of the mechanical structural loads and also offers ablative protection in the event of a heat-pipe failure.

The maximum operating temperature capability of coated refractory-composite materials for the primary structure of the leading edge is high (~3000°F) relative to refractory metals, which are typically limited to approximately 2400°F. The potentially

higher operating temperature increases the radiation heat-rejection efficiency of the heat-pipe-cooled leading edge and permits reductions in the mass of the leading edge for a given leading-edge radius. In addition, the higher operating temperature increases the total heat load that can be accommodated passively by the heat pipe (i.e., no forced convective cooling required). For many trajectories, the high operating temperatures help eliminate the need for active cooling during both ascent and descent, thus eliminating the need for carrying additional hydrogen fuel (coolant) into orbit. Since many hypersonic vehicles return unpowered for landing, the additional hydrogen fuel needed for cooling during descent would result in a mass penalty.

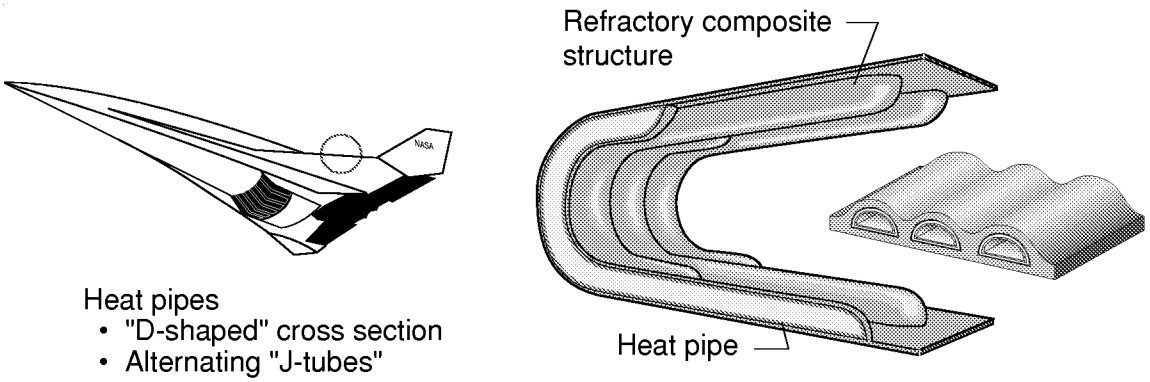

Figure 3: Schematic drawing of a hypersonic vehicle with a diagram of a heat-pipe-cooled wing leading edge.

Design Equations

The design of a heat-pipe-cooled leading edge is very complex due to the numerous variables involved. However, a simple set of closed form equations is presented here that can be used to determine if a heat-pipe-cooled leading edge is feasible with various material combinations. The equations presented here were developed to model the heat-pipe-cooled leading edge shown in Figure 3, but can be generalized for many other potential designs.

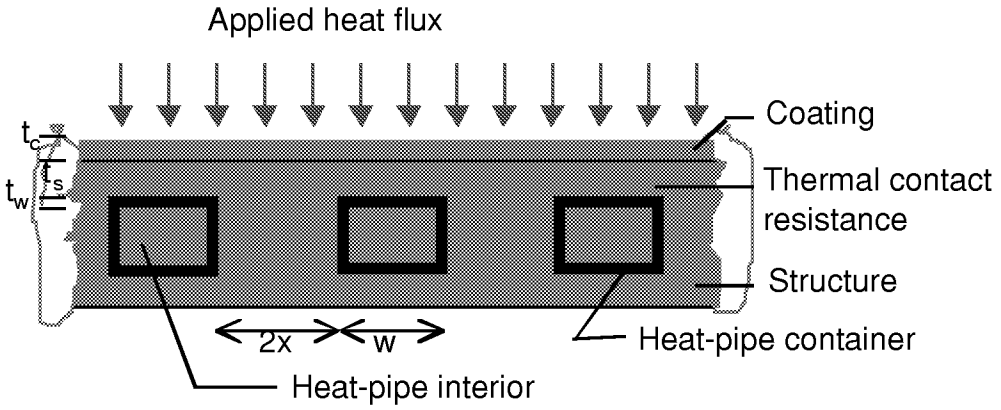

Figure 4: Schematic drawing of three heat pipes embedded in a structure.

Figure 4 shows a schematic cross-section diagram of three heat pipes embedded in a structural material. The heat pipes shown in the figure have a rectangular cross section, but other cross sections could be considered. The leading edge is subjected to aerodynamic heating on the outer surface. At the stagnation line - the location of maximum heating - the

heating rate is by denoted q''_{stag}. A coating of thickness t_c is placed on the outer surface of the structure. The thickness of the structure between the outer surface and the heat pipes is t_s and the heat-pipe container wall thickness is t_w. The distance between heat pipes is 2x, and the width of the heat pipe is w. Contact resistance between the structure and the heat pipe is also shown in the figure. The contact resistance on the other surfaces of the heat pipe is of much less concern and is thus neglected in this calculation.

The first step is to determine the temperature drop, ΔT_{stag}, through the structure and heat-pipe container at the stagnation line. This will help determine the maximum temperature of the leading edge, which will occur on the outer surface at the stagnation line midway between heat pipes. To determine the maximum temperature drop through the structure and heat-pipe container at the stagnation line, the following thermal resistances should be considered: through-the-thickness of the structure (from the outer surface to the heat pipe), in the plane of the structure (from midway between heat pipes to the heat pipe), and the contact resistance. If a coating is used on the outer surface, its thermal resistance (both in-plane and through-the-thickness) should be included. Two conduction paths are shown in Figure 5 for the heat conducted from midway between heat pipes on the outer surface to the heat pipe. As shown in Figure 5, the heat must be conducted through the coating and structure in the through-the-thickness direction, and through either the coating or structure in the in-plane direction.

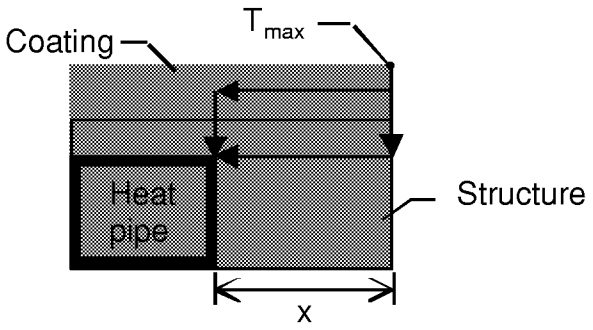

Figure 5: Schematic drawing of leading-edge cross section with heat pipe showing two potential paths for heat to be conducted from midway between heat pipes to a heat pipe.

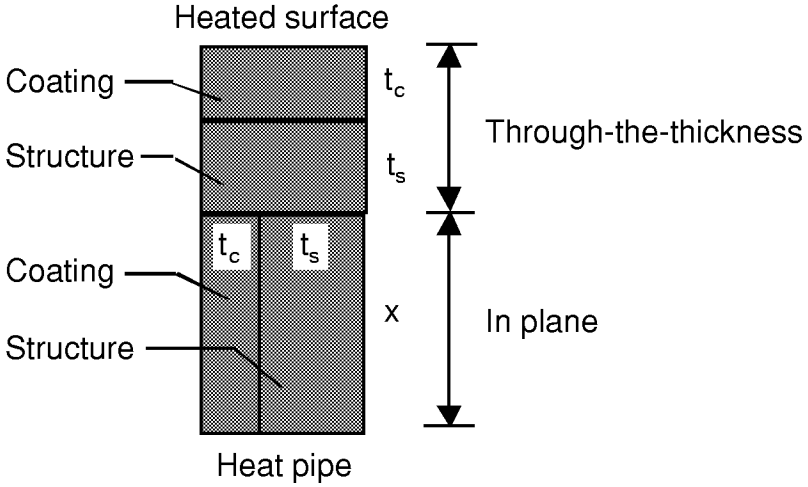

Figure 6: Schematic drawing of the series/parallel resistance network for heat to be conducted from midway between heat pipes on the outer surface to a heat pipe.

The drawing shown in Figure 6 is an attempt to approximate the 2-D geometry of Figure 5 with a 1-D thermal resistance network. The thermal resistance is for the heat conduction midway between heat pipes on the outer surface to the heat pipe. The through-the-thickness resistance in the structure is shown in Figure 6 prior to the in-plane resistances, but could be placed after the in-plane resistances with the same result. Other resistance networks could also be used, but care must be exercised due to inconsistent areas. The thermal resistance through the heat-pipe container is neglected since it is small relative to the other terms and since the heat transfer area is not consistent with the other terms. Contact resistance is not shown in Figure 6 due to its unknown value and area.

Knowing the stagnation heat flux, q''_{stag}, the dimensions, and the thermal conductivities, the temperature drop from a point midway between heat pipes on the outer surface to the heat pipe, ΔT_{stag}, can be determined from

$$q''_{stag} = \Delta T_{stag}/\Sigma R \tag{1a}$$

$$q''_{stag} = \frac{\Delta T_{stag}}{\frac{t_c}{k_c} + \frac{t_s}{k_{s,t}} + \left[\frac{k_{s,p} t_s/(t_s + t_c)}{x} + \frac{k_c t_c/(t_s + t_c)}{x}\right]^{-1}} \tag{1b}$$

The thermal resistance given in eq. (1b) is for the geometry shown in Figure 6, which was an attempt to approximate the 2-D geometry in Figure 5 with a 1-D thermal resistance approach. The first two terms represent the through-the-thickness series resistance through the coating and structure. The third term represents the in-plane parallel resistance through the coating and structure. The thickness ratios, $t_s/(t_s + t_c)$ and $t_c/(t_s + t_c)$, represent the cross sectional area (assuming a unit depth) for the heat conduction through each layer. Rearranging eq. (1b), the temperature drop can be obtained from

$$\Delta T_{stag} = q''_{stag} \left\{\frac{t_c}{k_c} + \frac{t_s}{k_{s,t}} + \left[\frac{x(t_s + t_c)}{k_{s,p} t_s + k_c t_c}\right]\right\} \tag{2}$$

The maximum value of the stagnation heat flux is used and the transient nature of the heating is not taken into account. Though this is a conservative approach, the thermal response of the leading edge will often be rapid enough that a steady state approximation at the time of maximum heating will provide relatively accurate temperatures.

The next step is to determine the average surface temperature based on the estimated heat-pipe length. To do this, one must know the heat-flux distribution and estimate the chordwise length of the heat pipes on both the upper and lower surface. (The heat pipes will normally be oriented perpendicular to the leading edge, referred to as the chordwise direction, but could be oriented in the flow direction. For a swept leading edge, orienting the heat pipes perpendicular to the leading edge results in easier fabrication and lower axial heat-pipe acceleration loads.) From the heat flux distribution, the integrated heat flux, q_{tot}, can be obtained for the entire chordlength, both upper and lower surface for a spanwise (parallel to the leading edge) unit width. The average outside surface temperature, T_{surf}, can then be estimated from

$$q_{tot} = \varepsilon \sigma A (T_{surf}^4 - T_{amb}^4) \tag{3}$$

Thermal radiation to the leading edge from the ambient is included in eq. (3), but can usually be neglected. Reducing the upper or lower length of the heat pipes, L_u or L_l respectively, will raise the average surface temperature. The area, A, is based on a 1-in-wide strip the total length of the heat pipe ($L_u + L_l$). It is important that the heat pipes extend past the stagnation region into the region where the maximum material reuse temperature is above the radiation equilibrium temperature. For sharp leading edges with small angles of attack, the heat flux drops off very rapidly, and should not be a problem. However, for very blunt leading edges with high angles of attack, high heat fluxes will extend a significant distance from the stagnation line.

The third step is to estimate the internal heat-pipe temperature. It is assumed that the heat pipe is at uniform temperature and that the heat radiated from the surface is also uniform. First, the heat flux out of the heat pipes is calculated assuming that the heat flux radiated from the leading-edge outer surface must first be conducted through the heat-pipe width, w. The distance between heat pipes is 2x and, thus, for every spanwise unit width of leading edge, the heat flux must be conducted through a heat-pipe of width w and is radiated from the outer surface over a width of w + 2x. Therefore, for each 1 in. unit width of leading edge, the heat is conducted to the outer surface through a width of

$$(1 \text{ in.})\ w/(w + 2x)$$

The average heat flux conducted through the wall of the heat-pipe container is then

$$q''_{avg} = \frac{q_{tot}}{(L_u + L_l)\ (1 \text{ in.})\ [w/(w+2x)]} \tag{4}$$

Knowing the average heat flux, the temperature drop through the structure and heat-pipe container, $\Delta T_{s,hp}$, can be obtained from

$$q''_{avg} = \frac{\Delta T_{s,hp}}{\frac{t_{s,t}}{k_{s,t}} + \frac{t_w}{k_w} + \frac{t_c}{k_c} + \frac{1}{h_{cr}}} \tag{5}$$

where the thermal resistance terms in eq. (5) are illustrated in Figure 7.

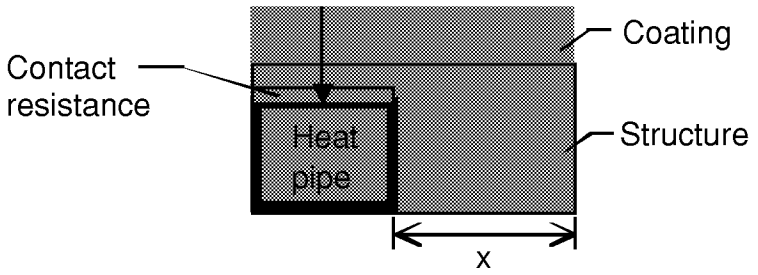

Figure 7: Schematic drawing of a leading-edge cross section with a heat pipe showing the four thermal resistance components (coating, structure, contact resistance, and heat-pipe container) in eq. (5).

Note that in eq. (5) there is no in-plane thermal resistance. Contact resistance between the heat pipe and structure, if known, can be included in eq. (5). If values of contact resistance can be estimated, it may also be possible to bound the problem. However, it should be

emphasized that thermal contact resistance is extremely dependent on geometry, pressure, material, and temperature.

The heat-pipe operating temperature is then obtained from

$$T_{hp} = T_{surf} - \Delta T_{s,hp} \tag{6}$$

The final value to obtain is the maximum leading-edge temperature, which will occur midway between heat pipes at the stagnation line. This temperature is obtained from

$$T_{max} = T_{hp} + \Delta T_{stag} \tag{7}$$

The important parameters for a heat-pipe-cooled leading edge have now been obtained: the maximum surface temperature, T_{max}, and the heat-pipe operating temperature, T_{hp}. A comparison of the calculated maximum surface temperature with the reuse temperature of the coating and structural materials will determine if they are feasible for this application. The heat-pipe operating temperature will help establish what container material and working fluid to use. Several iterations may be required to obtain a design with acceptable temperatures using the corresponding material properties. The dimensions used in the design, i.e., the length of the heat pipes on the upper and lower surfaces, the spacing between heat pipes, the width of the heat pipes, and all the thicknesses, can be modified to obtain alternate designs. In addition, different materials with different thermal properties can be evaluated. The goal is to obtain a design that results in temperatures within the reuse limits of available materials while utilizing dimensions that can be fabricated.

Comparison of Design and Finite Element Analysis Results

The use of the developed design equations are now illustrated for a blunt leading edge, and results for both a blunt and sharp leading edge are presented and compared with results from a 3-D finite element analysis.

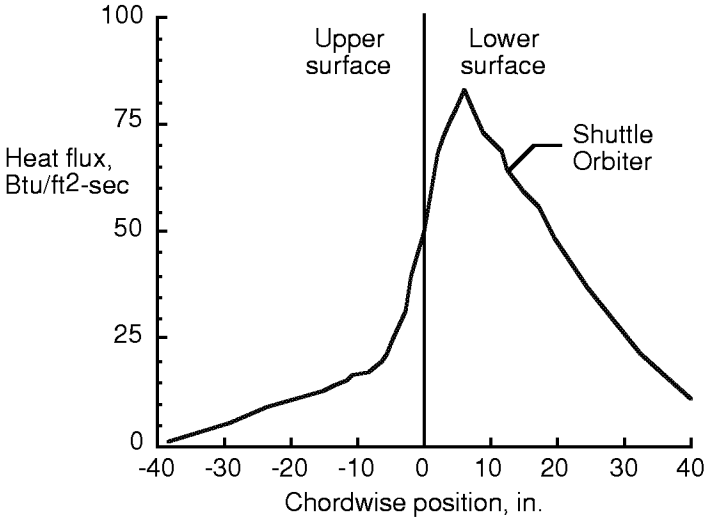

Figure 8: Typical heat flux distribution for Space Shuttle Orbiter wing leading edge.

As an example of the above procedure for a blunt leading edge, consider the Space Shuttle Orbiter wing leading edge with a stagnation heat flux of q''_{stag} = 83 Btu/ft^2-s and the chordwise (normal to the leading edge) heat flux distribution on the leading edge as shown

in Figure 8. Baseline (test case 1) dimensions and thermal conductivities are given in Table 1. An example of a spreadsheet used for the calculations is shown in Appendix A.

The temperature drop from the location at the outer stagnation line midway between heat pipes is given by eq. (2) as

$$\Delta T_{stag} = q''_{stag}\left\{\frac{t_c}{k_c}+\frac{t_s}{k_{s,t}}+\left[\frac{x(t_s+t_c)}{k_{s,p}t_s+k_c t_c}\right]\right\} \tag{2}$$

$$\Delta T_{stag} = 83\frac{Btu}{ft^2-s}\left\{\frac{0.01in.}{23.587\frac{Btu}{hr-ft-°F}}+\frac{0.04in.}{12.8\frac{Btu}{hr-ft-°F}}\right.$$

$$\left.+\frac{0.7in.(0.04in.+0.01in.)}{\left(24.408\frac{Btu}{hr-ft-°F}\right)(0.04in.)+\left(23.587\frac{Btu}{hr-ft-°F}\right)(0.01in.)}\right\} \tag{2}$$

$$\Delta T_{stag} = 807°F$$

Table 1: Baseline Variables for Comparison of Results

t_s	=	0.04 in.
t_w	=	0.01 in.
t_c	=	0.01 in.
x	=	0.7 in.
L_u	=	24 in.
L_l	=	18 in.
r	=	9 in.
$k_{s,t}$	=	12.8 Btu/hr-ft-°F
$k_{s,p}$	=	24.408 Btu/hr-ft-°F
k_w	=	39.485 Btu/hr-ft-°F
k_c	=	23.587 Btu/hr-ft-°F
ε	=	0.8

The next step is to estimate the average leading-edge surface temperature. The length on the upper surface is 24 in. and on the lower surface is 18 in. The total integrated heat load for a spanwise width of 1 in. and a chordwise length of 42 in. is 11.6 Btu/s. Since all of the heat must be reradiated, and neglecting radiation from the ambient, the average surface temperature can be calculated from

$$11.62\ Btu/s = \varepsilon\,\sigma\,A\,T_{surf}^{\ 4} = (0.8)\ (0.1714 \times 10^{-8}\ Btu/hr\text{-}ft^2\text{-}°R^4)\ (1\ in.)\ (42\ in.)\ T_s^{\ 4} \tag{3}$$

$$T_{surf} = 2738°F$$

The heat-pipe container width is 0.6 in. with a heat-pipe spacing (half the distance between heat pipes) of 0.7 in. Thus for every 1 in. of leading-edge width (spanwise direction), 11.62 Btu/s must be conducted to the outer surface through a width of

$$1\ in.\ [w/(w+2x)] = 0.3\ in.$$

The average heat flux conducted through the heat pipe to the outer surface is then

$$q''_{avg} = \frac{11.62 \text{Btu/s}}{(42\text{in.})(0.3\text{in.})} = 132.8 \text{ Btu/ft}^2\text{-s} \tag{4}$$

The thermal resistance from the coating, structure, and heat-pipe container are used to obtain the temperature drop through the leading edge. There is no in-plane thermal resistance included here since this is the region directly over a heat pipe.

$$132.8 \frac{\text{Btu}}{\text{ft}^2\text{s}} = \frac{\Delta T_{s,hp}}{\frac{0.04\text{in.}}{12.8 \frac{\text{Btu}}{\text{hr} - \text{ft} - °\text{F}}} + \frac{0.01\text{in.}}{39.485 \frac{\text{Btu}}{\text{hr} - \text{ft} - °\text{F}}} + \frac{0.01\text{in.}}{23.587 \frac{\text{Btu}}{\text{hr} - \text{ft} - °\text{F}}}} \tag{5}$$

$$\Delta T_{s,hp} = 151°\text{F}$$

Table 2: Comparison of Blunt Leading-Edge Temperatures

	$T_{hp,\ anal}$, °F	$T_{hp,\ FEA}$, °F	Difference, °F	$T_{max,\ anal}$, °F	$T_{max,\ FEA}$, °F	Difference, °F
Test case 1 q_{tot} = 11.6 Btu/s t_s = 0.04 in. x = 0.7 in. L_u = 24 in.	2587	2556	29	3394	3243	150
Test case 2 q_{tot} = 12.09 Btu/s t_s = 0.04 in. x = 0.05 in. L_u = 36 in.	2530	2420	110	2670	2505	165
Test case 3 q_{tot} = 11.6 Btu/s t_s = 0.25 in. x = 0.7 in. L_u = 24 in.	1933	2525	592	3145	3074	71
Test case 4 q_{tot} = 11.6 Btu/s t_s = 0.25 in. x = 0.05 in. L_u = 24 in.	2455	2537	82	3003	2821	182

With an average outer surface temperature of 2738°F and a temperature drop through the structure of 151°F, the heat-pipe temperature is given as

$$T_{hp} = T_{surf} - \Delta T_{s,hp} = 2738°\text{F} - 151°\text{F} = 2587°\text{F} \tag{6}$$

The maximum leading-edge temperature is the sum of the heat-pipe operating temperature and the temperature drop from the location midway between heat pipes to the heat pipe, given by

$$T_{max} = T_{hp} + \Delta T_{stag} = 2587°F + 807°F = 3394°F \quad (7)$$

A comparison of the heat-pipe temperature and maximum surface temperature are summarized in Table 2 for the 1-D design equations and a full 3-D finite element analysis (FEA) for a blunt leading edge such as on the Space Shuttle Orbiter. A discussion of the FEA is presented in Appendix B. Though the FEA has a nonlinear property capability, the constant properties in Table 1 were used in the FEA to provide a true comparison with the design equations. In each case, the variables that are different from those in Table 1 are listed in the table (all other variables are the same as in Table 1). For all cases in Table 2, q_{stag} = 83 Btu/ft^2-s and r = 9 in.

Table 3: Comparison of Sharp Leading-Edge Temperatures

	$T_{hp, anal}$, °F	$T_{hp, FEA}$, °F	Difference, °F	$T_{max, anal}$, °F	$T_{max, FEA}$, °F	Difference, °F
Test case 5 q_{tot} = 19.142 Btu/s t_s = 0.04 in. x = 0.05 in. $L_u = L_l$ = 24 in.	2968	3036	68	4230	4077	153
Test case 6 q_{tot} = 22.906 Btu/s t_s = 0.04 in. x = 0.05 in. $L_u = L_l$ = 36 in.	2791	2851	60	3962	3926	127
Test case 7 q_{tot} = 19.142 Btu/s t_s = 0.04 in. x = 0.7 in. $L_u = L_l$ = 24 in.	2826	2985	159	10,121	6064	4057

Test cases 1-4 are for a blunt leading edge (r = 9 in.) with a relatively low heat flux and a large angle of attack (see Figure 8). Test case 2 has a much smaller half heat-pipe spacing than in test case 1 (0.05 in. vs. 0.7 in. in test case 1) and a longer upper surface heat-pipe length. The longer upper surface heat pipe results in a slightly larger integrated heat load. In test case 3, the thickness of the structure beneath the coating is increased to 0.25 in. and the half spacing between heat pipes is 0.7 in. Both of these dimensions are relatively large and result in a heat-pipe temperature that is quite low. The combination of a thick structure above the heat pipe and a relatively large distance between heat pipes results in a large thermal resistance, and thus a large temperature difference, between the outer surface and the heat pipe. The larger dimensions also result in the 1-D approximation being less accurate. In test case 4, the structural thickness is still large, but the heat pipes are spaced much closer, and the heat-pipe temperature from the design equations is much closer to that from the FEA.

Three cases are presented for a sharp leading edge (r = 0.5 in.) with a higher heat flux (q_{stag} = 750 Btu/ft^2-s) in Table 3. The angle of attack for test cases 5-7 is near zero. The design results compare well with the FEA except for large heat-pipe spacing (test case 7), where the maximum temperatures obtained by the two methods are very different. This is due to the fact that as the heat-pipe spacing increases, the problem becomes more three dimensional, and the design equations become less accurate. However, both the design equations and the FEA indicate that the design with a large heat-pipe spacing is not feasible.

Discussion

Since a heat pipe redistributes thermal energy instead of removing it as in active cooling, the total energy balance is extremely important. For this reason, sharp leading edges are much more conducive to heat-pipe cooling than blunt leading edges. A blunt leading edge, though it will have a lower stagnation heat flux than a sharp leading edge under the same flow conditions, may have a higher integrated heat load. As a result, the surface area required to radiate the energy away may be larger, i.e. longer heat pipes are required.

Low angles of attack are more conducive to heat-pipe cooling than high angles of attack. A high angle of attack will heat a larger portion of the lower surface, making it less useful for radiating away heat transferred from the stagnation region. The heat must thus be moved to the upper surface which experiences very little heating. The required heat-pipe lengths are then much longer than for a correspondingly low angle of attack leading edge.

The approximation for the design analyses presented here conservatively estimates the maximum temperatures by assuming no transfer of heat chordwise at the stagnation line. In Figure 4, the 2-D geometry is approximated as a 1-D problem. However, due to the sharp reduction in heat flux at the stagnation line, three dimensions should be considered for a complete analysis. For sharp leading edges, heat will be transferred away from the stagnation line in the chordwise direction parallel to the heat pipes, thus reducing the leading-edge temperatures and resulting in a conservative approximation. For blunt leading edges, the chordwise heat flux reduction is much less, and the three dimensional effect is correspondingly less significant.

A second conservative feature in the developed design analysis (and the FEA) is the use of a constant applied heat flux on the outer surface with only radiation losses. In actual aerodynamic heating, the reduction in the applied heat flux with rising surface temperature is much greater if convection to a hot surface is considered rather than assuming a constant heat flux with radiation losses alone. This effect is most pronounced as the heat-pipe spacing increases. For a very small heat-pipe spacing, the surface temperature, and thus heat flux, is relatively uniform. For a large heat-pipe spacing, the maximum temperature between heat pipes is much greater than directly over a heat pipe. If surface temperature dependent convective aerodynamic heating is considered instead of a constant applied heat flux, the aerodynamic heating applied to the surface will decrease significantly with the rise in surface temperature. This results in a "damping" of the temperature rise. The design equations presented here can thus be used to evaluate feasibility assuming closely spaced heat pipes. Once it is determined that heat pipes are feasible with closely spaced heat pipes, a more detailed analysis should be utilized to determine optimum heat-pipe spacing.

Concluding Remarks

A set of closed form equations have been presented to quickly evaluate the feasibility of utilizing heat pipes to cool leading edges of hypersonic vehicles. The results from the

design equations were compared with results from a 3-D FEA for both a large and small radius leading edge. The results compared quite well and indicate that the equations can be used for a quick assessment of the feasibility of using heat pipes to cool a leading edge. If feasibility is indicated, a more detailed analysis should follow.

Acknowledgment

The author would like to thank the Thermal Structures Branch at NASA Langley Research Center for funding this work under Contract No. NAS1-96014.

References

[1]Silverstein, C. C., "A Feasibility Study of Heat-Pipe-Cooled Leading Edges for Hypersonic Cruise Aircraft," NASA CR 1857, Nov. 1971.

[2]Niblock, G. A., Reeder, J. C., and Huneidi, F., "Four Space Shuttle Wing Leading Edge Concepts," *Journal of Spacecraft and Rockets*, Vol. 11, No. 5, 1974, pp. 314-320.

[3]Alario, J. P., and Prager, R. C., "Space Shuttle Orbiter Heat Pipe Application," NASA CR 128498, April 1972.

[4]Anon., "Study of Structural Active Cooling and Heat Sink Systems for Space Shuttle," NASA CR 123912, June 1972.

[5]Anon., "Design, Fabrication, Testing, and Delivery of Shuttle Heat Pipe Leading Edge Test Modules," NASA CR 124425, April 1973.

[6]Camarda, C. J., "Analysis and Radiant Heating Tests of a Heat-Pipe-Cooled Leading Edge," NASA TN D-8468, Aug. 1977.

[7]Camarda, C. J., "Aerothermal Tests of a Heat-Pipe-Cooled Leading Edge at Mach 7," NASA TP-1320, Nov. 1978.

[8]Camarda, C. J., and Masek, R. V., "Design, Analysis and Tests of a Shuttle-Type Heat-Pipe-Cooled Leading Edge," *Journal of Spacecraft and Rockets*, Vol. 18, No. 1, 1981, pp. 71-78.

[9]Peeples, M. E., Reeder, J. C., and Sontag, K. E., "Thermostructural Applications of Heat Pipes," NASA CR 159096, June 1979.

[10]Boman, B. L., Citrin, E. C., Garner, E. C., and Stone, J. E., "Heat Pipes for Wing Leading Edges of Hypersonic Vehicles," NASA CR 181922, Jan. 1990.

[11]Boman, B. L., and Elias, T., "Tests on a Sodium/Hastelloy X Wing Leading Edge Heat Pipe for Hypersonic Vehicles," AIAA Paper 90-1759, June 1990.

[12]Merrigan, M. A., Sena, J. T., and Glass, D. E., "Evaluation of a Sodium/Hastelloy-X Heat Pipe Designed to Cool the Wing Leading Edge of an Advanced Space Transportation System", Proceedings of the ASME Heat Transfer Conference, Houston, TX, August 1996, pp. 333-341.

[13]Glass, D. E., and Camarda, C. J., "Preliminary Thermal/Structural Analysis of a Carbon-Carbon/Refractory-Metal Heat-Pipe-Cooled Wing Leading Edge," *Thermal Structures and Materials for High Speed Flight,* edited by E. A. Thornton, Vol. 140, Progress in Astronautics and Aeronautics, AIAA, Washington, DC, 1992, pp. 301-322.

[14]Glass, D. E., Camarda, C. J., Sena, J. T., and Merrigan, M. A., "Fabrication and Testing of Heat Pipes for a Heat-Pipe-Cooled Leading Edge," AIAA 97-3876, August 1997.

[15]Glass, D. E., Merrigan, M. A., and Sena, J. T., "Fabrication and Testing of Mo-Re Heat Pipes Embedded in Carbon/Carbon," NASA/CR-1998-207642, March 1998.

[16]Whetstone, W. D., EISI-EAL Engineering Analysis Language Reference Manual - EISI-EAL System Level 2091, Engineering Information Systems, Inc., July 1983.

Appendix A: Spreadsheet Description

A spreadsheet was used to determine the temperatures using the design equations. An example of the spreadsheet used in shown in Table 4 for test case 2. Rows 2-15 are the input variables, many of which were listed in Table 1. For the thermal conductivity and heat flux per unit area, the values given in column D have the units listed with the definition in column B. The values in column E have the units listed in column F. Rows 17-21 are the output values. The parameter, along with its units, is listed in column B and the calculated value is listed in column C. The equations used to calculate the values in column C are given in column D.

Table 4: Spreadsheet Showing Leading-Edge Temperature Calculations

A/1	B	C	D	E	F
2	t structure, in.			0.04	
3	t wall, in.			0.01	
4	t coating, in.			0.01	
5	half hp spacing, in.			0.05	
6	L upper, in.			36	
7	L lower, in.			18	
8	k structure, t-t, Btu/hr-ft-°F		12.8	0.000296	Btu/in-s-°F
9	k structure, plane, Btu/hr-ft-°F		24.408	0.000565	Btu/in-s-°F
10	k wall, Btu/hr-ft-°F		39.485	0.000914	Btu/in-s-°F
11	k coating, Btu/hr-ft-°F		23.587	0.000546	Btu/in-s-°F
12	emittance			0.8	
13	q stag, Btu/ft2-s		83	0.576	Btu/in2-s
14	qtot, integrated heat load, Btu/s			12.09	
15	heat-pipe width, in.			0.6	
16					
17	R	242.41	=E4/E11 + E2/E8 + E5*(E2+E4)/(E2*E9 + E4*E11)		
18	ΔT stag, °F	140	=E13*C17		
19	Tsurf, °F	2573	=(E14*3600*144/(E12*0.000000001714*(E6+E7)))^0.25 - 460		
20	ΔThp, °F	43	=((E14/((E6+E7)*(E15/(E15+2*E5)))))*(E2/E8 + E3/E10 + E4/E11)		
21	Thp, °F	2530	=C19-C20		
22	Tmax, °F	2670	=C21+C18		

Appendix B: Finite Element Analysis

A three-dimensional, thermal finite element model was used to obtain the finite element solutions to compare with the design results. A schematic diagram of the leading edge is shown in Figure 9. The shaded region in the figure represents surfaces of the 3-D region that was modeled in the analysis. The Engineering Analysis Language (EAL) system was used to perform the finite element analysis.[16] The model was constructed using the executive control language in EAL in a very general sense, in that the physical dimensions of the leading edge, the composite architecture, and the boundary conditions can be easily varied.

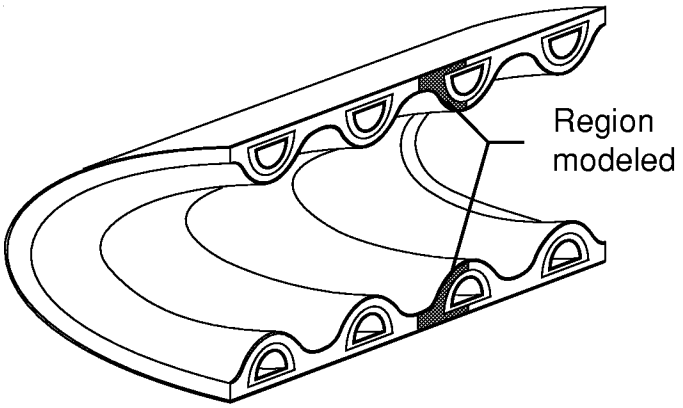

Figure 9: Schematic drawing of a wing leading edge showing surfaces of the 3-D region modeled in the finite element analysis.

Elements were clustered near the stagnation region in the chordwise direction where the heat flux and temperature gradients are the largest. Element clustering was used in the chordwise direction since the chordwise dimension is much larger than the spanwise or through-the-thickness dimensions. The transformation used to concentrate the elements in the stagnation region in the chordwise direction is a logarithmic clustering algorithm given by

$$y = B + \frac{1}{\tau} \sinh^{-1}\left[\left(\frac{p}{z} - 1\right)\sinh(\tau B)\right] \tag{8}$$

where

$$B = \frac{1}{2\tau} \ln\left[\frac{1+(e^{\tau}-1)(z/s)}{1+(e^{-\tau}-1)(z/s)}\right], \quad 0 < \tau < \infty \tag{9}$$

and where y is the transformed coordinate in the chordwise direction along the leading edge, p the original equally spaced coordinate, z the point about which the clustering occurs, and s the heat-pipe length. The stretching parameter τ can be varied to space the points equally (small τ) or to concentrate the points near z (large τ). In the spanwise and through-the-thickness directions a linear grid was used. A typical finite element model used for the comparison is shown in Figure 10. In the figure, the chordwise length is much smaller than the actual case, but the number of elements is representative of those used in the analysis.

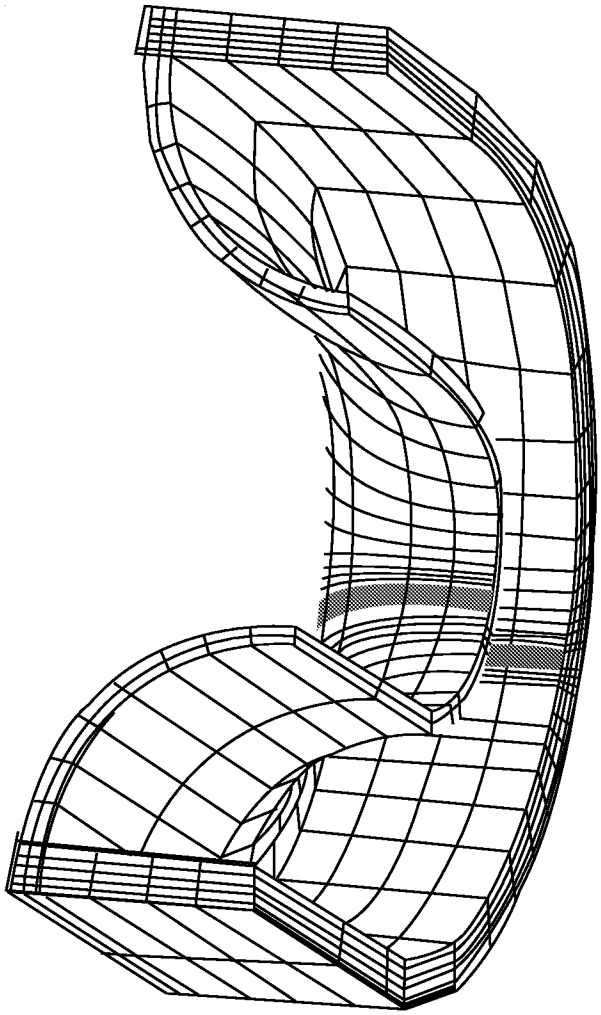

Figure 10: Finite element model of section of leading edge modeled.

The walls of the heat pipes were modeled by three-dimensional conduction elements and the internal vapor temperature was modeled by an isothermal surface on the inner surface of the heat pipe to simulate an infinite thermal conductivity for the heat pipe. This was a nonconservative assumption, and detailed heat-pipe analyses are necessary to determine actual temperature drops along the heat pipe. However, it is a good assumption for high-temperature liquid metal heat pipes.

The cross-sectional finite element grid used in the model is shown in Figure 11 along with the boundary conditions. Radiation exchange between the hot leading edge and a cool ambient is insignificantly different than if the ambient is assumed to be at absolute zero, and thus heat is radiated from the external surface to space at absolute zero. (This assumption is non-conservative, but has a negligible impact on the surface temperatures with high aerodynamic heating.) An insulated internal surface was considered since all interior surface temperatures are relatively uniform. The heated surface and the surfaces cooled by radiation are shown in Figure 11. The surface midway between the chordwise heat pipes and the surfaces through the center of the chordwise heat pipe are assumed to be thermally insulated as a result of symmetry.

Several simplifying assumptions were made in the finite element analysis. Perhaps the largest uncertainty in the thermal finite element analysis is the assumption of perfect

thermal contact between the carbon-carbon structure and the heat pipes. It is known that thermal contact resistance will result in increased surface temperatures in the stagnation region, but since no value for the contact resistance is known, its quantitative effect on the temperatures is uncertain. It is anticipated that, upon heating, the thermal expansion of the heat pipe would increase the contact pressure between the heat pipe and structure, thereby reducing the thermal contact resistance.

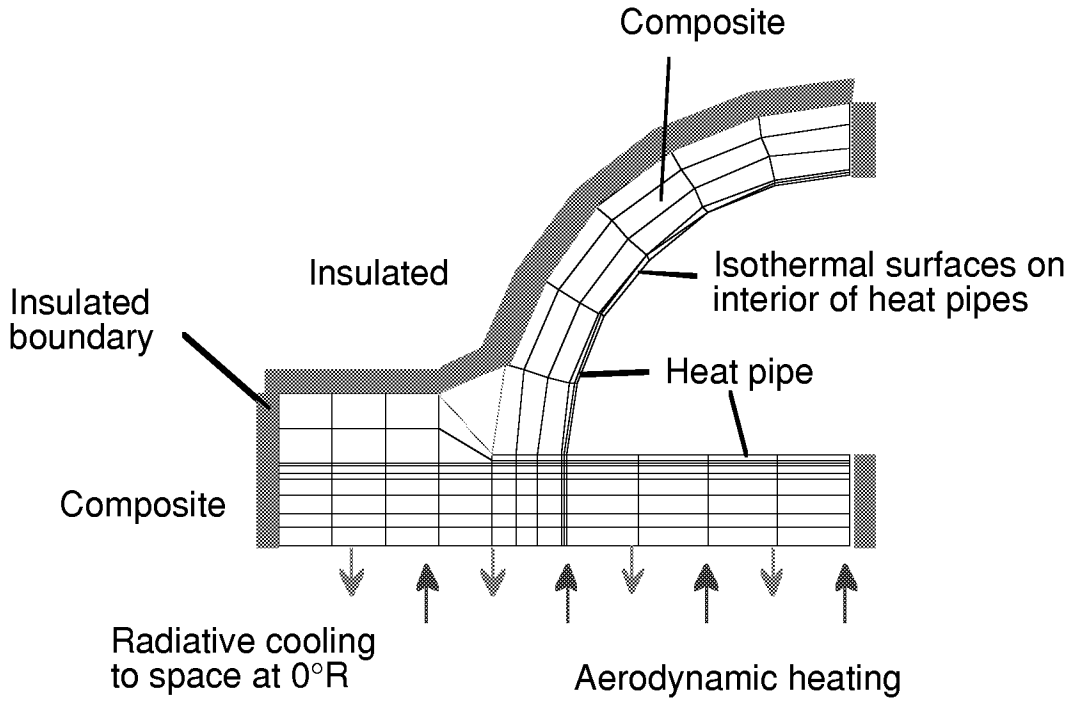

Figure 11: Boundary conditions used in the finite element analysis.

REPORT DOCUMENTATION PAGE

Form Approved
OMB No. 0704-0188

1. AGENCY USE ONLY (*Leave blank*)	2. REPORT DATE	3. REPORT TYPE AND DATES COVERED
	December 1998	Contractor Report

4. TITLE AND SUBTITLE
Closed Form Equations for the Preliminary Design of a Heat-Pipe-Cooled Leading Edge

5. FUNDING NUMBERS
NAS1-96014
WU 242-33-03-20

6. AUTHOR(S)
David E. Glass

7. PERFORMING ORGANIZATION NAME(S) AND ADDRESS(ES)
Analytical Services & Materials, Inc.
107 Research Drive
Hampton, VA 23669-1340

8. PERFORMING ORGANIZATION REPORT NUMBER
AS&M-LS15-98-01

9. SPONSORING/MONITORING AGENCY NAME(S) AND ADDRESS(ES)
National Aeronautics and Space Administration
Langley Research Center
Hampton, VA 23681-2199

10. SPONSORING/MONITORING AGENCY REPORT NUMBER
NASA/CR-1998-208962

11. SUPPLEMENTARY NOTES
This report was prepared by Analytical Services & Materials, Inc., under subcontract to Lockheed Martin Engineering & Sciences, Hampton, Virginia, under NASA Contract NAS1-96014 to Langley Research Center.
Langley Technical Monitor: Stephen J. Scotti
An electronic version of this report can be found at: http://techreports.larc.nasa.gov/ltrs

12a. DISTRIBUTION/AVAILABILITY STATEMENT
Unclassified-Unlimited
Subject Category 34 Distribution: Nonstandard
Availability: NASA CASI (301) 621-0390

12b. DISTRIBUTION CODE

13. ABSTRACT *(Maximum 200 words)*

A set of closed form equations for the preliminary evaluation and design of a heat-pipe-cooled leading edge is presented. The set of equations can provide a leading-edge designer with a quick evaluation of the feasibility of using heat-pipe cooling. The heat pipes can be embedded in a metallic or composite structure. The maximum heat flux, total integrated heat load, and thermal properties of the structure and heat-pipe container are required input. The heat-pipe operating temperature, maximum surface temperature, heat-pipe length, and heat pipe-spacing can be estimated. Results using the design equations compared well with those from a 3-D finite element analysis for both a large and small radius leading edge.

14. SUBJECT TERMS	15. NUMBER OF PAGES
Heat pipes, leading edges	23
	16. PRICE CODE: A03

17. SECURITY CLASSIFICATION OF REPORT	18. SECURITY CLASSIFICATION OF THIS PAGE	19. SECURITY CLASSIFICATION OF ABSTRACT	20. LIMITATION OF ABSTRACT
Unclassified	Unclassified	Unclassified	